CRYSTAL GROWTH & DESIGN

Article

Evidence for Halogen Bonding in Amorphous Solid Dispersions

Chailu Que, Qingqing Qi, Dmitry Y. Zemlyanov, Huaping Mo, Alexandru Deac, Matthias Zeller, Anura S. Indulkar, Yi Gao, Geoff G.Z. Zhang, and Lynne S. Taylor

Cryst. Growth Des., **Just Accepted Manuscript** • DOI: 10.1021/acs.cgd.0c00073 • Publication Date (Web): 20 Mar 2020

Evidence for Halogen Bonding in Amorphous Solid Dispersions

Chailu Que,[1] Qingqing Qi,[2] Dmitry Y. Zemlyanov,[3] Huaping Mo,[4] Alexandru Deac,[1] Matthias Zeller,[2] Anura S. Indulkar,[5] Yi Gao,[6] Geoff G. Z. Zhang,[5] and Lynne S. Taylor*[1]*

1. Department of Industrial and Physical Pharmacy, College of Pharmacy, Purdue University, West Lafayette, Indiana 47907, United States

2. Department of Chemistry, College of Science, Purdue University, West Lafayette, Indiana 47907, United States

3. Birck Nanotechnology Center, Purdue University, West Lafayette, Indiana 47907, United States

4. Purdue Interdepartmental NMR Facility, Department of Medicinal Chemistry and Molecular Pharmacology, Purdue University, West Lafayette, Indiana 47907

5. Drug Product Development, Research and Development, AbbVie Inc., North Chicago, Illinois 60064, United States

6. Science and Technology, Operations, AbbVie Inc., North Chicago, Illinois 60064, United States

Corresponding authors: *Geoff G. Z. Zhang (Telephone: +1-847-937-4702; Fax: +1-847-937-7756) and *Lynne S. Taylor (Telephone: +1-765-496-6614; Fax: +1-765-494-6545).

E-mail addresses: Geoff.GZ.Zhang@abbvie.com (G.G.Z. Zhang), lstaylor@purdue.edu (L.S. Taylor)

Abstract

Carbon-bound halogen atoms (iodine, bromine, chlorine and occasionally fluorine) are known to act as electron acceptors and form interactions with different species capable of acting as electron donors. This interaction is termed halogen bonding, and shares some similarities with hydrogen bonding. While hydrogen bonding has been extensively studied as an important intermolecular interaction for many aspects drug delivery and dosage form design, halogen bonding has not been investigated in these contexts. However, approximately one third of all drug molecules contain halogen atoms. Using X-ray photoelectron spectroscopy, nuclear magnetic resonance spectroscopy, and infrared spectroscopy, it was demonstrated herein that halogen-bearing drugs that lack hydrogen bond donors form a halogen bonding interaction with the carbonyl group of a common pharmaceutical polymer, copovidone, in a solid amorphous blend. Halogen bonding thus may be a common, but neglected intermolecular interaction in drug-polymer amorphous blends, and potentially important for the properties and performance of these systems which are used to enhance drug solubility and delivery. This is the first time that the occurrence of halogen bonding has been observed in drug-polymer formulations.

Keywords

Amorphous solid dispersions, halogen bonding, X-ray photoelectron spectroscopy, nuclear magnetic resonance, infrared spectroscopy

1. Introduction

Drugs are rarely delivered to the body in pure form. Instead, highly engineered dosage forms are necessary in order for the drug to reach its intended site of action at the right dose and rate. Of the many challenges in drug delivery, poor aqueous solubility of modern drug candidates is one of the most prevalent issues.[1, 2] Miscible blends of a lipophilic drug with a hydrophilic polymer, termed amorphous solid dispersions (ASDs), are one of the most popular formulation strategies for oral delivery of poorly soluble drugs. It is widely recognized that using an ASD formulation can greatly improve drug bioavailability relative to the crystalline form.[3, 4] The intermolecular interactions between drug and polymer are considered critical to ASD formulation performance.[5-8] One of the most frequently studied intermolecular interactions in ASDs is hydrogen bonding. Several studies have suggested that hydrogen bonding helps delay drug crystallization in the solid state,[9-11] maintain the supersaturation generated by dissolving an ASD,[12] and potentially can improve dissolution performance.[6] In contrast, halogen bonding, another noncovalent interaction, has not been investigated for these drug formulations.

Halogen bonding (XB) is the attractive interaction between the electrophilic region of halogen (F, Cl, Br, I) substituents and Lewis bases. Even though halogen atoms have the capability to donate a lone pair of electrons, the electrophilic region on the halogen atoms, termed the σ hole, and located *trans* to its σ bond, can attract electron-rich sites, such as oxygen, nitrogen, and halogen atoms.[13] Considering the fact that both halogen bond donors and acceptors are electronegative, the existence of halogen bonding is somewhat counterintuitive. According to a survey of ligand-protein interactions from the Protein Data Bank, the most common element acting as electron donor in halogen bonds are carbonyl oxygen atoms, followed by nitrogen.[14, 15] Although it has been only approximately a half century since halogen bonding was first

demonstrated by Hasselt in 1960s,[16] this interaction has been explored and exploited in many fields including crystal engineering,[17, 18] material science,[19] protein-ligand interactions,[20, 21] supermolecular gel formation,[22] and catalysis.[23, 24] Halogen bonding also has been used to form pharmaceutical co-crystals to modify the physicochemical properties of active pharmaceutical ingredients and excipients.[25-27] In general, the strength of the halogen bond depends on the size of the σ-hole, following the trend of I > Br > Cl > F.[13] However, the strength can be tuned by changing the chemical environment of the halogens, e.g. by adding electron donating or withdrawing substituents in the vicinity of the carbon atom attached to the halogens. Among the halogens, F is the least prone to be involved in halogen bonding, only forming halogen bonds when fluorine atoms in the vicinity to strong electron-withdrawing groups.[28] Halogen bonds tend to be directional, and the ideal C—X···A contact angle between the σ-hole and the halogen bond acceptor A is close to 180°.[29] For optimized systems, the strength of the halogen bond can be comparable to that of a hydrogen bond.[13] In a study of protein-ligand complexes, the interaction energies for halogen bonds were estimated to range from -1.97 to -5.4 kcal/mol, where the stronger halogen bonds have comparable interaction energies as a typical hydrogen bond.[30] For example, the interaction energy of the hydrogen bond between hydroxyl in methanol and carbonyl in acetone is about -5.3 kcal/mol.[31] It has been shown in several crystal engineering studies that when both intermolecular interactions are available, hydrogen bonding is favored over halogen bonding, but that both interactions can co-exist.[18, 32] Another interesting characteristic of halogen bonding is that it tends to be less sensitive to, and persists in a polar environment.[29, 33]

The most frequently used experimental technique for studying halogen bonding is X-ray crystallography, which enables measurement of the interatomic distance between halogen donor

and acceptor.[34] However, this technique can only be applied to crystalline materials. Other techniques, such as solid and solution state nuclear magnetic resonance (NMR),[33, 35] infrared (IR) spectroscopy,[36] Raman spectroscopy,[37] and X-ray photoelectron spectroscopy (XPS)[19] have been employed to characterize halogen bonding. Density functional theory (DFT) calculations are often used to confirm experimental observations of halogen bonding.[38]

Investigations into halogen bonding are gaining traction, and the occurrence of such interactions in drug formulations is of considerable relevance given that more than 30% of the drug molecules in development contain halogens, and halogen bonds have been observed in a variety of biomolecular systems.[14] Medicinal chemists have taken advantage of halogen bonding in the design of new therapeutics.[20, 39] However, the implications of halogen bond formation in drug formulation has been ignored. Of particular interest in this context, are interspecies interactions for halogen-bearing drugs dispersed in polymers. Polymers are widely used in drug formulations, and play a pivotal role in the formation of ASDs, a solubility enhancing platform for low aqueous solubility drugs.[40] While several types of intermolecular drug-polymer interactions have been described previously including hydrogen bonding and ionic interactions,[10, 41-43] halogen bonds in these systems have not been reported to date.

In the current study, we chose four model compounds that contain Cl, Br or I, but lack hydrogen bond donors (shown in Figure 1), where clotrimazole and loratadine are marketed drugs. Brotrimazole is a derivative of clotrimazole obtained by replacing Cl with Br. Compound 3, 3-bis(3,5-diiodo-4-methoxyphenyl)isobenzofuran-1(3H)-one (Me-DIBF) is a methylated derivative of a protein inhibitor.[44] The polymers investigated (Figure 1) were copovidone (PVPVA), which is present in many important commercial ASD formulations,[40] and the somewhat simpler, but closely related polymer, povidone (PVP). To demonstrate and investigate halogen bonding

between model compounds and polymers, X-ray photoelectron spectroscopy was used to monitor changes in the electronic environment of relevant atoms. Solution nuclear magnetic resonance spectroscopy was used to measure the binding strength between donor and acceptor. Lastly, infrared spectroscopy was used to provide confirmation of the acceptor group. For the first time, the presence of drug-polymer halogen bonding is demonstrated in amorphous formulations.

2. Materials

Clotrimazole (Figure 1a) was purchased from Sigma-Aldrich (St. Louis, MO, USA). Loratadine (Figure 1c) was attained from Attix Pharmaceuticals (Toronto, ON, Canada). Compound 3,3-bis(3,5-diiodo-4-methoxyphenyl)isobenzofuran-1(3H)-one (Me-DIBF) and 1-((2-bromophenyl)diphenylmethyl)-1H-imidazole, (brotrimazole), shown in Figure 1b and 1d respectively, were synthesized in-house, and the synthesis procedures are described in detail in the methods section. Copovidone (PVPVA) 64 (Figure 1e) and povidone (PVP K29-32) (Figure 1f) were obtained from Ashland (Covington, KY). Deuterated toluene, containing 0.03 % (v/v) tetramethylsilane (TMS), deuterated cyclohexane, TMS, 1-ethylpyrrolidine (Figure 1g), 1-ethyl-2-pyrrolidone (Figure 1h) were all purchased from Sigma-Aldrich (St. Louis, MO, USA). Ethanol 200 proof anhydrous, tetrahydrofuran (THF), and all the chemicals for synthesis were bought from Fisher Scientific (Hampton, NH, USA).

(a) (b)

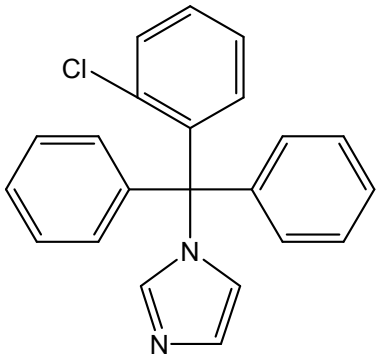
Cl
N
N

(c)

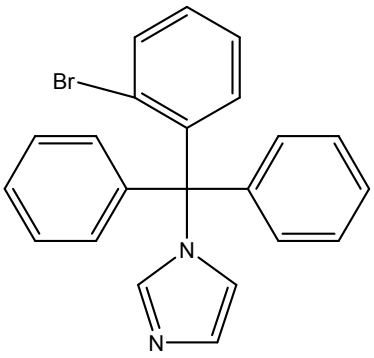
Br
N
N

(d)

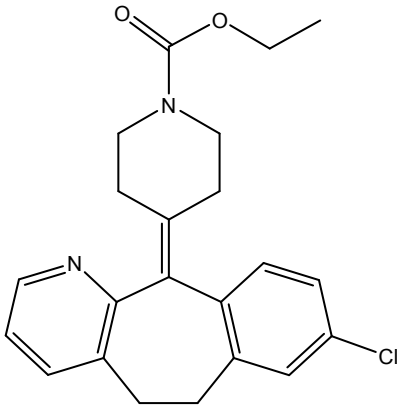
O
O
N
N
Cl

(e)

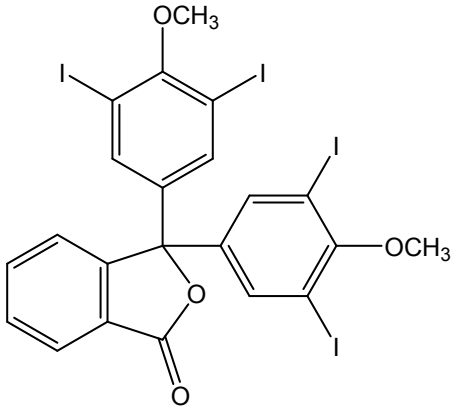
OCH3
I
I
I
OCH3
O
I
O

(f)

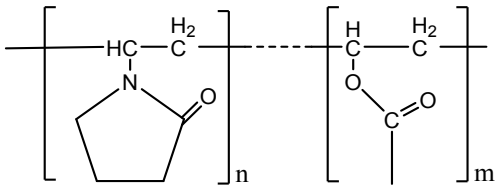
H2
HC
C
N
O
n
H
C
H2
C
O
O
C
m

(g)

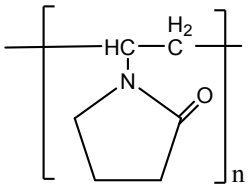
H2
HC
C
N
O
n

(h)

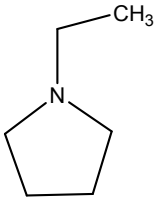
CH3
N

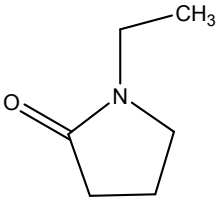
CH3
O
N

Figure 1. Molecular structure of (a) clotrimazole, (b) brotrimazole, (c) loratadine, (d) 3,3-bis(3,5-diiodo-4-methoxyphenyl)isobenzofuran-1(3H)-one (Me-DIBF), (e) PVPVA , (f) PVP, (g)1-ethylpyrrolidine, and (h) 1-ethyl-2-pyrrolidone.

3. Experiments

3.1 Synthesis of Brotrimazole

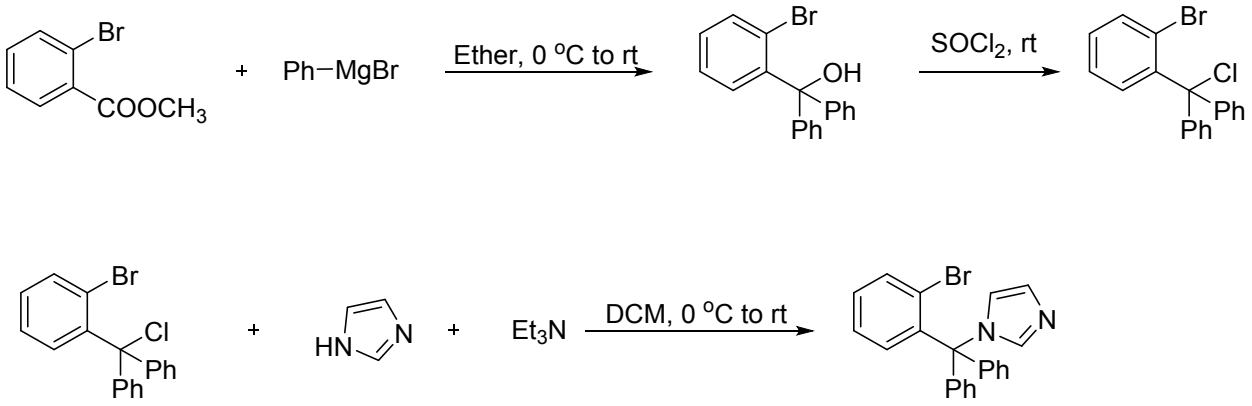

Scheme 1. Synthesis of brotrimazole (1-((2-Bromophenyl)diphenylmethyl)-1*H*-imidazole).

(2-Bromophenyl)diphenylmethanol The preparation was as described previously[45]: to a stirred solution of methyl 2-bromobenzoate (2.6 g, 12 mmoL, 1.0 equiv) in anhydrous Et_2O (40 mL) at 0 ^oC under nitrogen was added PhMgBr (8.8 mL, 3.0 M in Et_2O, 2.2 equiv). The reaction mixture was stirred at room temperature overnight. The reaction was quenched by sat. NH_4Cl solution (7 mL). The mixture was extracted by Et_2O, the organic layers were combined and the solvent was removed under vacuum. The residue was purified by silica gel chromatography with hexane as the eluent to afford the product as white solid (3.5 g, 86%).

((2-Bromophenyl)chloromethylene)dibenzene (2-bromophenyl)diphenylmethanol (3.4 g, 10.0 mmol, 1.0 equiv) was mixed with $SOCl_2$ (10 mL, excess) and several drops of DMF were added. The mixture was stirred at room temperature overnight. The stirring was stopped upon the completion of reaction as monitored by ^1H NMR of the crude mixture. Then $SOCl_2$ was removed

under vacuum. To the residue was added DCM (5 mL) and the solution was concentrated in volume again and this was repeated for three times to afford ((2-bromophenyl)chloromethylene)dibenzene which was used directly in the next step without further purification.

Brotrimazole (1-((2-Bromophenyl)diphenylmethyl)-1*H*-imidazole) To a precooled solution of 2-bromophenyl)chloromethylene)dibenzene (10.0 mmol, 1.0 equiv) in anhydrous DMF (20 mL) at 0 °C under argon was added 1*H*-imidazole (1.0 g, 15.0 mmol, 1.5 equiv) and triethylamine (4.2 mL, 30.0 mmol, 3.0 equiv) via a syringe. The reaction mixture was allowed to warm to room temperature and stirred overnight. 50 mL ethyl acetate was added and the solution was washed with brine for three times, and dried over Na_2SO_4. After filtration and concentration, the crude mixture was purified by column chromatography (silica gel, 50% ethyl acetate in hexanes) to afford the title product (3.0 g, 77.1%). ^{1}H NMR (800 MHz, Chloroform-*d*) δ 7.66 (dd, *J* = 7.9, 1.5 Hz, 1H), 7.49 (t, *J* = 1.2 Hz, 1H), 7.36 – 7.32 (m, 6H), 7.30 – 7.28 (m, 1H), 7.24 – 7.21 (m, 5H), 7.07 (d, *J* = 1.3 Hz, 1H), 6.91 (dd, *J* = 8.0, 1.7 Hz, 1H), 6.76 (d, *J* = 1.5 Hz, 1H). ^{13}C NMR (201 MHz, $CDCl_3$) δ 142.19, 140.36, 139.24, 135.90, 130.93, 130.52, 129.86, 128.46, 128.17, 127.97, 127.56, 125.90, 121.63. HRMS (m/z, APCI): calcd for $C_{22}H_{18}BrN_2$(M+H)+: 389.0653. Found: 389.0639. ^{1}H and ^{13}C NMR spectra for the final product are provided in the supporting information.

3.2 Synthesis of 3,3-bis(3,5-diiodo-4-methoxyphenyl)isobenzofuran-1(3H)-one (Me-DIBF)

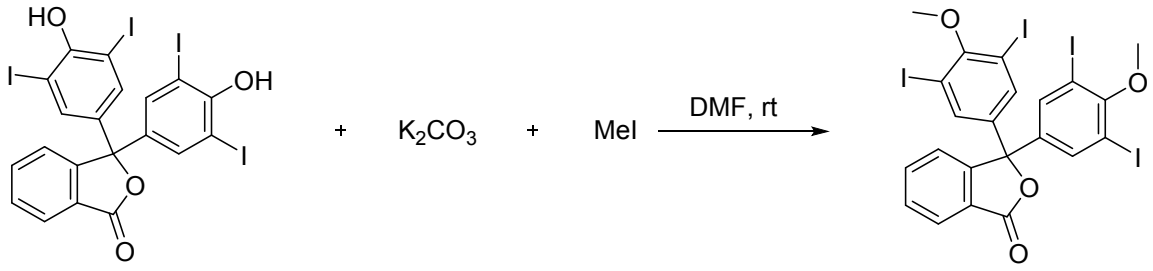

Scheme 2. Synthesis of 3,3-bis(3,5-diiodo-4-methoxyphenyl)isobenzofuran-1(3H)-one (Me-DIBF).

To a solution of 3,3-bis(4-hydroxy-3,5-diiodophenyl)isobenzofuran-1(3H)-one (6.6 g, 8.0 mmol, 1.0 equiv) in anhydrous DMF (50 mL) at RT under argon was added K_2CO_3 (4.4 g, 32.0 mmol, 4.0 equiv) and MeI (2.5 mL, 40.0 mmol, 5.0 equiv) via a syringe. The reaction mixture was stirred overnight. The mixture was poured into water and filtered to afford the title product as a white solid (6.5g, 95.6%). ^{1}H NMR (800 MHz, Chloroform-*d*) δ 8.00 – 7.98 (m, 1H), 7.83 – 7.81 (m, 1H), 7.69 – 7.65 (m, 5H), 7.58 – 7.56 (m, 1H), 3.88 (s, 6H). ^{13}C NMR (201 MHz, $CDCl_3$) δ 168.44, 159.52, 149.85, 139.44, 138.09, 134.97, 130.31, 126.72, 125.09, 123.78, 91.01, 87.36, 60.73. HRMS (m/z, ESI): calcd for $C_{22}H_{15}I_2O_4$(M+H)+: 850.7149. Found: 850.7137. ^{1}H and ^{13}C NMR spectra for the final product are shown in the supporting information.

3.3 Single Crystal X-ray Structure Determination

Crystallization and Data Collection

Single crystals were grown from a solution of dichloromethane and ethyl acetate using hexane vapor diffusion. Two crystals were selected for data collection and analyzed to ensure reproducibility of results. The crystals were mounted on a Mitegen micromesh mount using a trace of mineral oil and cooled to 150 K. Data were collected on a Bruker D8 Quest Single Crystal CMOS Diffractometer (Bruker, Nano Inc, Madison, WI) with a sealed tube X-ray source generating Mo-Kα radiation (λ = 0.71073 Å), a curved triumph monochromator with a 10 cm x 10 cm Photon-100 detector and fixed chi angle, and an Oxford Cryostream 800 plus variable temperature device (80-500K). Reflections were collected and processed, and the data was corrected for absorption and scaled by the multi-scan method using the Apex3 software v2018.1-0 (Bruker Nano Inc, Madison, WI).

Structure Determination and Refinement

The space group was assigned and the structure was solved using XPREP within the SHELXTL suite of programs[46, 47] by direct methods. Structure refinement was performed in SHELXL version 2018/3[48, 49] by full matrix least squares on F^2 with all reflections. Hydrogen atoms attached to carbons were geometrically placed in calculated positions and were constrained to ride on their parent atoms, such that the hydrogen-carbon bond distance for the aromatic C-H was 0.95 Å. U_{iso}(H) values for the C-H units were set to be a 1.2 multiple of U_{eq}(C). The imidazole and one of the phenyl groups were refined as disordered. The imidazole was refined in three parts such that two imidazole moieties were placed in similar positions but rotated 180^0 againstone another, while the position of the third imidazole moiety was swapped with the position of one of the phenyl rings. Similarly, the phenyl ring was refined in three parts such that two phenyl moieties were placed in similar positions but slightly shifted, coinciding with the rotation of the imidazole, while the position of the third phenyl moiety was swapped with the third imidazole moiety. U^{ij} components of all thermal parameters were restrained to be similar to each other. The bond distance between the central carbon atom and the carbon atom on the disordered phenyl ring was restrained to be similar to the bond distance between the central carbon atom and the carbon atom of one of the non-disordered phenyl rings for all disordered phenyl moieties. Similarly, the bond distance between the central carbon atom and the nitrogen for the minor moieties was restrained to be similar to that for the major moiety. Lastly, the diffraction intensities were corrected for extinction. Complete crystallographic data, in CIF format, have been deposited with the Cambridge Crystallographic Data Center: CCDC 1964776. Additional crystal data, data collection and refinement details can be found in the supporting information. The data can be obtained free of charge from The Cambridge Crystallographic Data Centre via. www.ccdc.cam.ac.uk/datarequest/cif.

3.4. Preparation of Amorphous Solid Dispersions (ASDs)

All amorphous solid dispersions were prepared by solvent evaporation using a rotatory evaporator (Brinkman Instruments, Westbury, NY). The organic solvent used to dissolve both drug and polymer was ethanol, except for Me-IDBF, where tetrahydrofuran was used. The temperature of the water bath was 60 °C and 40 °C for ethanol and tetrahydrofuran, respectively. Subsequently, the ASDs were placed in a vacuum oven for a day to remove residual organic solvent. Clotrimazole-PVPVA, clotrimazole-PVP, and loratadine-PVPVA ASDs were prepared with drug loadings of 10, 20, 25, 30, 40 and 50 wt. %. Brotrimazole-PVPVA and Me-DIBF-PVPVA ASDs were prepared with drug loading of 10, 20, 30 and 40 wt. %.

3.5 X-ray Photoelectron Spectroscopy (XPS)

XPS data were obtained by a Kratos Axis Ultra DLD spectrometer using monochromic Al Kα radiation (1486.6 eV). The spectra was collect at constant pass energy (PE) at 20 and 160 eV for high-resolution and survey spectra, respectively. A commercial build-in Kratos charge neutralizer was used to avoid non-homogeneous electric charge of non-conducting powder and to achieve better resolution. All the ASD samples for XPS were compressed into tablets prior to examination. 100 mg ASD powder were compressed at 1500 psi using a hydraulic press (Carver Inc, Wabash, IN) in a round die with diameter of 8 mm, and the compression pressure was held for 60s. Then the tablets were ejected manually from the die. The tablet were placed on a stainless steel sample holder bar using a double-sided sticking Cu tape. The XPS spectra were collected at 5 different points for each tablet. The size of analysis spots was 0.5 mm in diameter. XPS data were analyzed with the CasaXPS software (www.casaxps.com). Prior to data analysis, the C-C component of the C 1s peak was set to a binding energy (BE) of 284.8 eV to correct for charge at each acquisition spot. Curve-fitting was performed following a Shirley background

subtraction using Gaussian/Lorentzian peak shapes. The atomic concentrations of the elements in the near-surface region were estimated after a Shirley background subtraction taking into account the corresponding Scofield atomic sensitivity factors and inelastic mean free path (IMFP) of photoelectrons using standard procedures in the CasaXPS software assuming homogeneous mixture of the elements within the information depths (~10 nm).

3.6 Nuclear Magnetic Resonance (NMR) Spectroscopy

^{1}H and ^{13}C NMR were performed using Bruker Avance-III-800 spectrometer (Billerica, MA) equipped with a QCI cryoprobe. Titration was used to obtain binding constants. Deuterated cyclohexane was chosen as a solvent to ensure sufficient solute solubility and to avoid interference with halogen bonding. Chemical shifts were reported relative to tetramethylsilane (TMS). All samples were equilibrated at 25 °C for at least 5 min before data collection. To evaluate the weak interaction between drug or its analogues and 1-ethylpyrrolidinone (which is a monomeric analogue of PVP and maintains good solubility in toluene), we monitored model compound chemical shifts by EP titrations. The general procedure for titrations was as follows: a deuterated toluene stock solution with the host compound (concentration of 14.5 mM) was divided amongeight NMR tubes (0.6 mL each). A variable amount of 1-ethyl-2-pyrrolidone (EP) as guest was added to each tube to provide a range of halogen bonding acceptor concentrations. The guest concentrations used were 11.0, 87.5, 173.2, 339.9, 654.6, 946.8 and 1218.9 mM for each titration sample. The chemical shift of the host molecule was monitored and the titration curves were fitted to a 1:1 binding model, which is a hyperbolic function, using OriginPro 2019 (Originlab Corporation, Northampton, MA) to determine the binding constant K_F, which is given by equation 1:

$$K_F = \frac{[AD]}{[A][D]} \quad (1)$$

where [AD] is the concentration of the halogen-bonded complex, while [A] and [D] are the concentrations of the free acceptor and the free donor, respectively.

Using NMR spectroscopic titration to attain binding constants is a widely used approach.[33, 50-52] Titrations were repeated three times for reproducibility and estimation of errors, one set of representative NMR spectra and the titration curves for each model compound are presented here. The binding constants were determined by both ^{1}H NMR and ^{13}C NMR. For control experiments, 1-ethylpyrrolidine, which lacks the carbonyl group present in 1-ethylpyrrolidinone, was added to the host solution to examine its impact on the chemical shift.

3.7 Bulk Infrared (IR) Spectroscopy

Thin films of pure PVPVA, clotrimazole-PVPVA mixtures, brotrimazole-PVPVA mixtures, and Me-DIBF-PVPVA mixtures were spin-coated on thallium bromoiodide (KRS-5) windows (Harrick Scientific Corporation, Ossining, NY) using a spin coater (Chemat Technology Inc., Northridge, CA). The general procedure for spin coating was as follows: 50 μL of the PVPVA or drug-PVPVA ethanol solution with solid content of 100 mg/mL was deposited onto the substrate, then it was spun for 15 s at 50 rpm followed by 50 s at 2500 rpm. The IR spectra were collected using a Bruker Vertex 70 FTIR spectrometer (Bruker, Billerica, MA). For each sample, 128 scans were collected for both background and samples at a resolution of 4 cm^{-1}. The data were analyzed utilizing the OPUS software (version 7.2, Bruker Billerica, MA). IR spectra for loratadine-PVPVA were not collected due to the overlap of the carbonyl group in loratadine with PVPVA carbonyl group region.

4. Results

4.1 X-ray Photoelectron Spectroscopy (XPS)

The chemical composition of all the neat model compounds and ASDs was analyzed using XPS. The binding energies of the Cl 2p electrons in clotrimazole and loratadine, the Br 3d electrons in brotrimazole, and the I 3d electrons in Me-DIBF were measured respectively. The 2p and 3d core-level spectra are characterized by spin-orbit splitting, and therefore show two components. The ratios between the two components are 2:1 and 3:2 for p and d orbitals, respectively. The spin-orbit splitting for Cl 2p, Br 3d, and I 3d are 1.6, 1.0 and 11.5 eV respectively. The Cl 2p spectrum of pure clotrimazole exhibits one pair of peaks at 200.4 ± 0.1 (Cl $2p_{3/2}$) and 202.0 ± 0.1 eV (Cl $2p_{1/2}$) as shown in Figure 2a. However, when the clotrimazole molecules were dispersed into PVPVA, two new pairs of Cl peaks at 198.1 ± 0.2 (Cl $2p_{3/2}$), 199.8 ± 0.2 (Cl $2p_{1/2}$) and 196.7 ± 0.4 (Cl $2p_{3/2}$), 198.3 ± 0.1 eV (Cl $2p_{1/2}$) emerged (Figure 2a). Similar results were obtained for clotrimazole and PVP (Figure 2b). The Cl 2p peaks for loratadine showed a similar pattern, where two extra pairs of Cl 2p peaks with lower binding energy emerged in ASDs (Figure 2 d). The Br 3d spectrum from neat brotrimazole also showed an extra pair of photoelectron peaks with lower binding energy, corresponding to a 25% atomic ratio. The probable explanation is presence of two energetically similar molecular conformations of brotrimazole (see Figure 5S). This possibility is supported by crystal structure refinement of pure brotrimazole, which revealed disorder of the imidazole and phenyl substituents switching positions 18% of time, resulting in Br interacting with a phenyl ring instead of imidazole. In general, the phenyl ring is a better electron donating group. Therefore, the portion of Br atoms with a lower binding energy are likely a result of Br interacting with a phenyl ring instead of imidazole. In contrast, in the ASD matrix, Br 3d peaks, occurring at lower binding energies of 67.1 ± 0.1, 68.1 ± 0.1 eV, were dominant (Figure 2c). In Figure 2e, the neat Me-DIBF compound showed only one pair of I 3d photoelectron peaks with binding energy of 620.7 ± 0.1 (I $3d_{5/2}$), 632.2 ± 0.1 eV (I $3d_{1/2}$) eV,

while an extra pair of peaks at 618.1 ± 0.1 and 629.6 ± 0.1 eV were observed in the ASDs. Binding energies for all systems are summarized in Table 2. For each of these compounds, which contained different halogen atoms, the halogen atom showed additional lower binding energy peaks in the XPS spectrum when the compounds were molecularly mixed with PVPVA or PVP. A binding energy shift to a lower energy is an indication that the atom has become more electron-rich. Thus, in the ASD matrix, the halogen atoms likely received electrons from carbonyl groups present in the polymers, PVPVA or PVP.

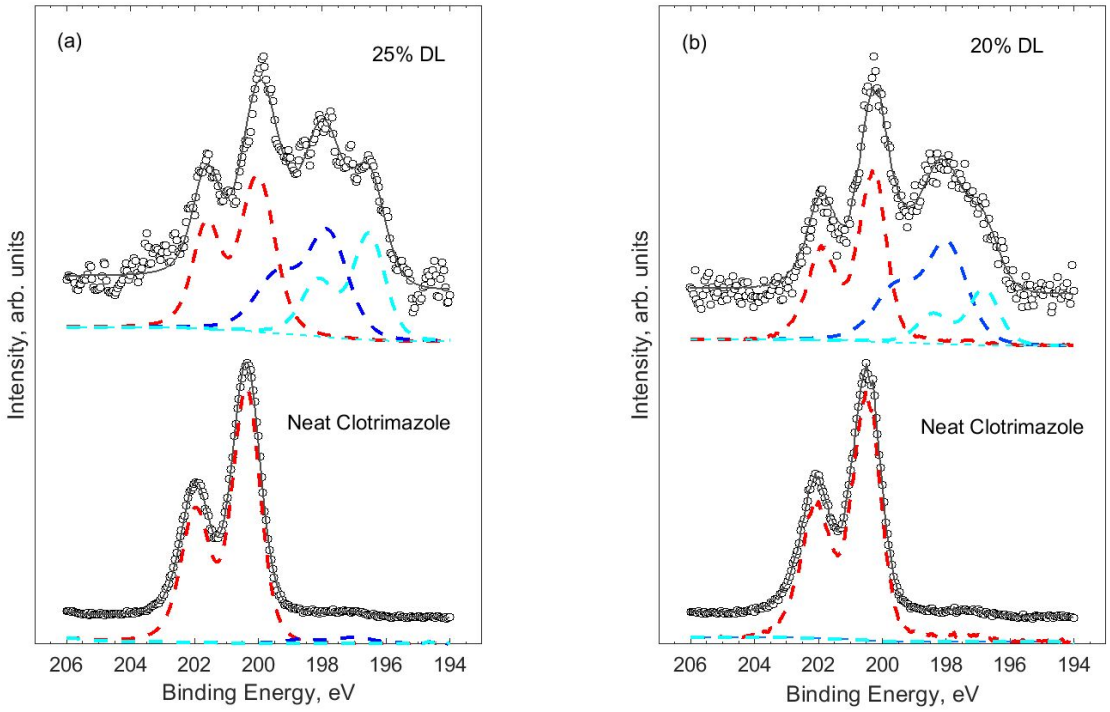

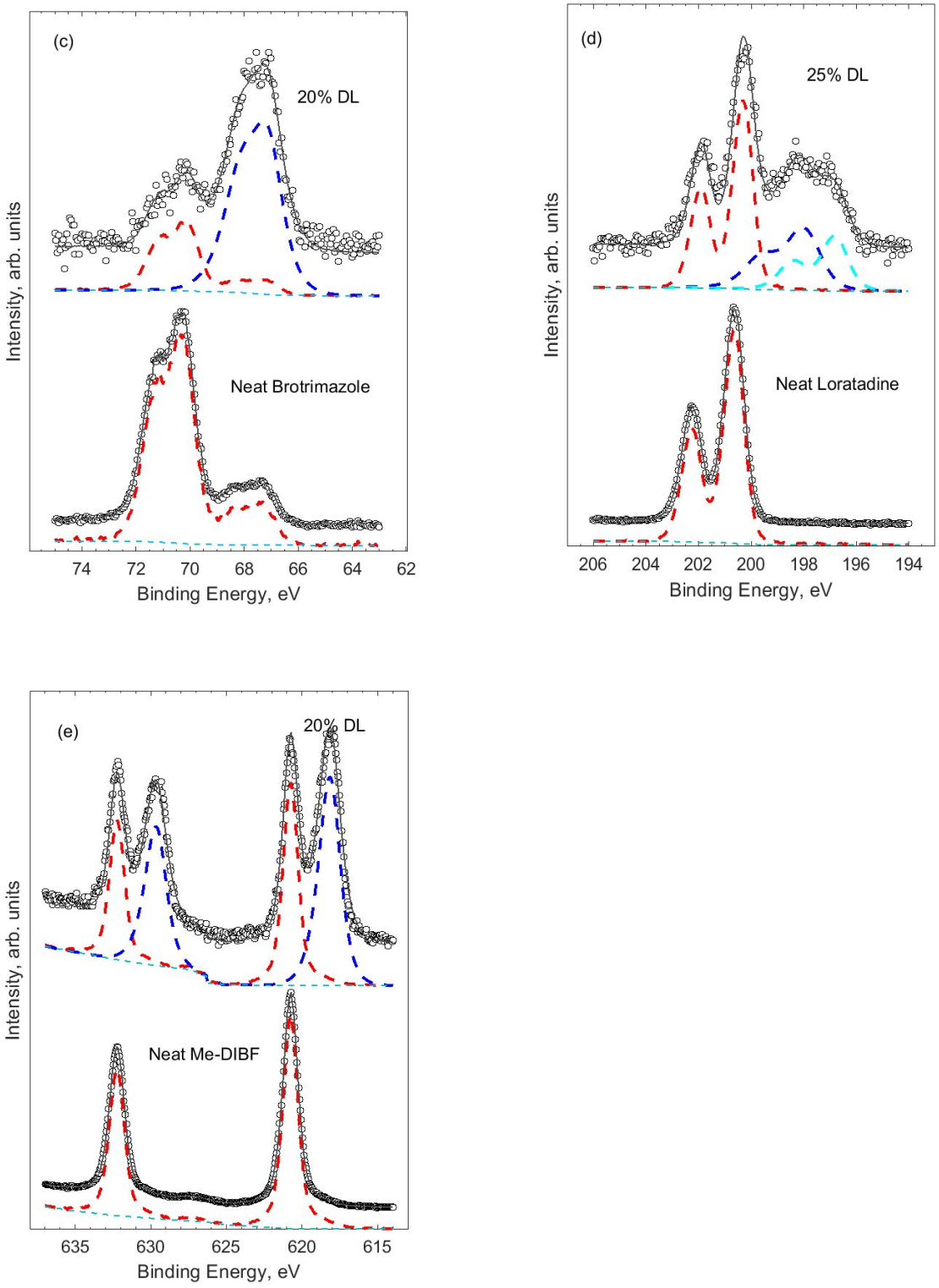

Figure 2. **Representative halogen X-ray photoelectron spectrum for (a) clotrimazole/PVPVA ASDs, (b) clotrimazole/PVP K29-32 ASDs, (c) brotrimazole/PVPVA ASDs, (d) loratadine/PVPVA ASDs, and (e) Me-**

DIBF/PVPVA ASDs. The X-ray photoelectron spectrum of neat model compound were also shown for comparison.

Table 1. Binding energy for neat materials and for peaks shifted to lower binding energies when dispersed in polymers.

	Neat Compound (eV)	Low Binding Energy Peaks when Dispersed in Polymer (eV)
Clotrimazole (PVPVA)	200.4 ± 0.1, 202.0 ± 0.1	198.1 ± 0.2, 199.8 ± 0.2 196.7 ± 0.4, 198.3 ± 0.4
Clotrimazole (PVP K29-32)	200.4 ± 0.1, 202.0 ± 0.1	197.9 ± 0.1, 199.5 ± 0.1 196.8 ± 0.1, 198.4 ± 0.1
Brotrimazole (PVPVA)	70.3 ± 0.1, 71.2 ± 0.1	67.1 ± 0.1, 68.1 ± 0.1
Loratadine (PVPVA)	200.6 ± 0.04, 202.2 ± 0.1	198.0 ± 0.1, 199.6 ± 0.1 196.8± 0.0, 198.4 ± 0.0
Me-DIBF (PVPVA)	620.7 ± 0.1, 632.2 ± 0.1	618.1 ± 0.1, 629.6 ± 0.1

By deconvoluting the XPS spectra, the percentage of halogen atoms showing low binding energy peaks was calculated for different drug loadings, with results summarized in Figure 3 and numerical values of the percentage of the lower binding energy peaks given in Table S2. We rationalized that at low drug loading, the drug molecules are further apart, and hence a majority have a higher tendency to interact with polymer. In contrast, at high drug loading, the drug molecules are in closer proximity to each other, and a majority have a greater likelihood of self-interactions. The trend among all ASDs is that the percentage of halogen atoms possessing a lower binding energy decreased as the drug load increased. This supports the idea that PVPVA is donating electrons to the halogens.

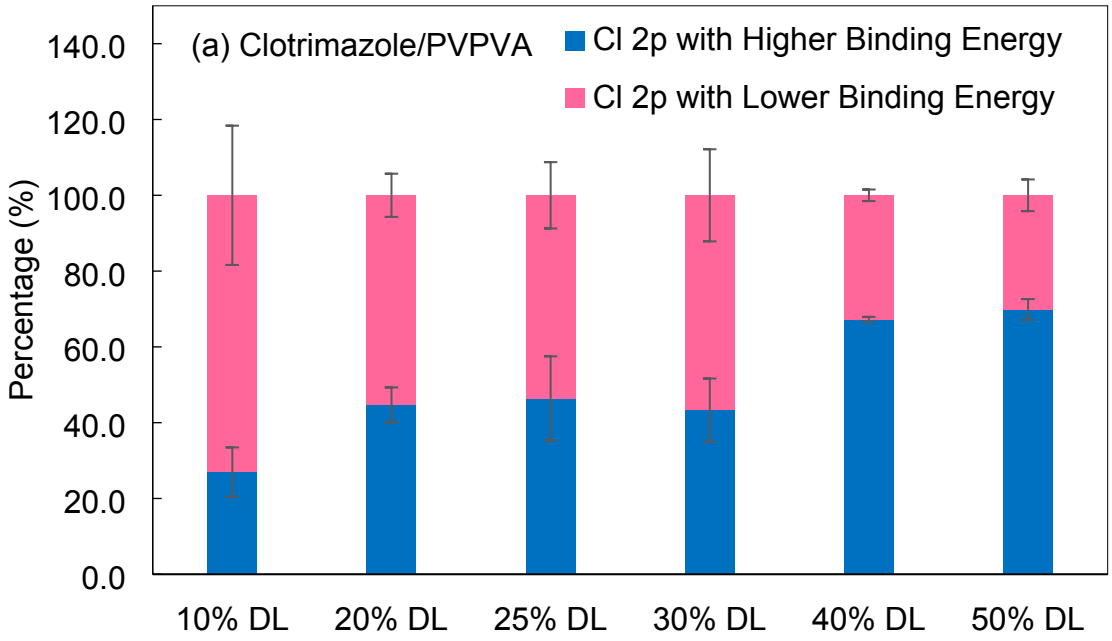
(a) Clotrimazole/PVPVA
Cl 2p with Higher Binding Energy
Cl 2p with Lower Binding Energy
Percentage (%)
140.0
120.0
100.0
80.0
60.0
40.0
20.0
0.0
10% DL
20% DL
25% DL
30% DL
40% DL
50% DL

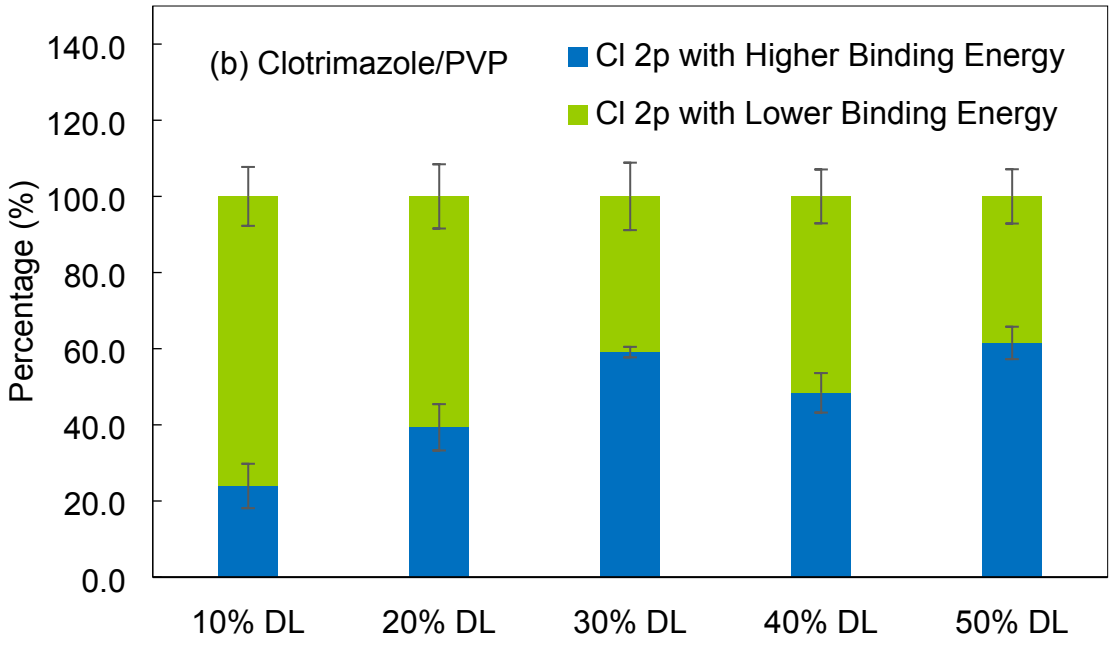
(b) Clotrimazole/PVP
Cl 2p with Higher Binding Energy
Cl 2p with Lower Binding Energy
Percentage (%)
140.0
120.0
100.0
80.0
60.0
40.0
20.0
0.0
10% DL
20% DL
30% DL
40% DL
50% DL

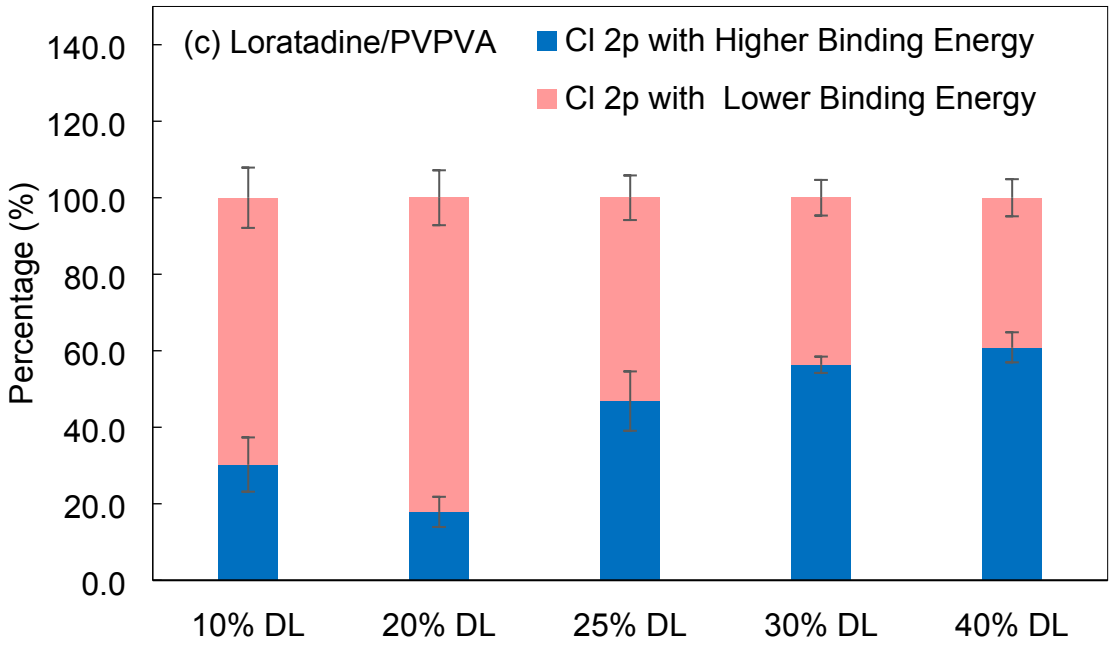
(c) Loratadine/PVPVA
Cl 2p with Higher Binding Energy
Cl 2p with Lower Binding Energy
Percentage (%)
140.0
120.0
100.0
80.0
60.0
40.0
20.0
0.0
10% DL
20% DL
25% DL
30% DL
40% DL

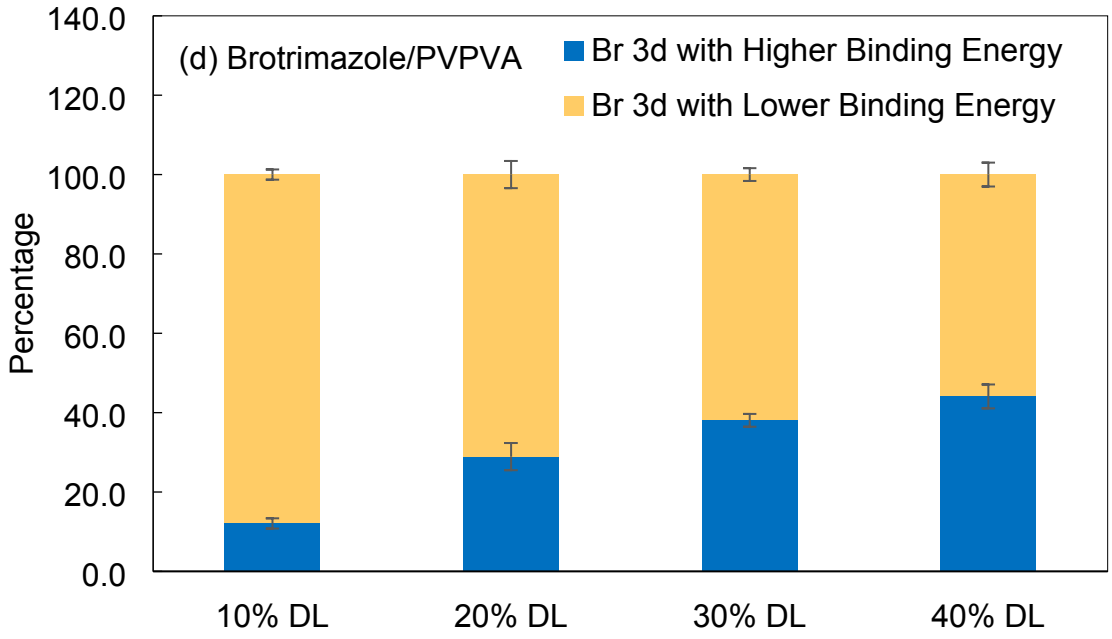
(d) Brotrimazole/PVPVA
Br 3d with Higher Binding Energy
Br 3d with Lower Binding Energy
Percentage
140.0
120.0
100.0
80.0
60.0
40.0
20.0
0.0
10% DL
20% DL
30% DL
40% DL

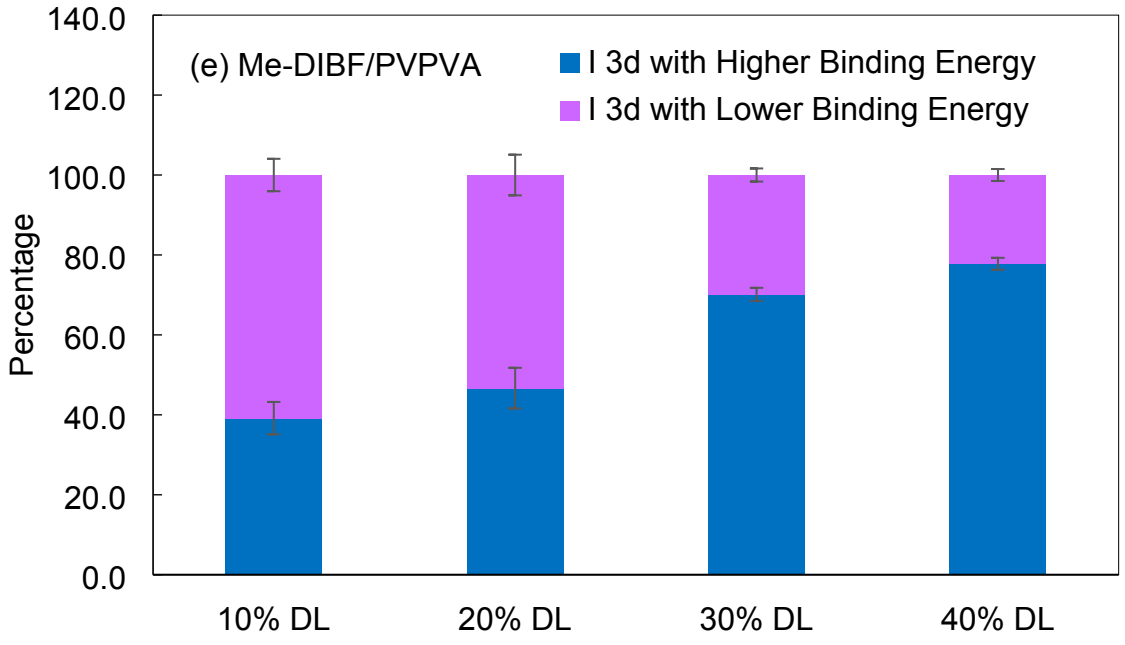

Figure 3. **The percentage of halogen atoms with high (as found in the neat compound) and low binding energies (new peaks seen in the ASD) as a function of wt. % drug loading (DL) in the ASD for ASD system (a) clotrimazole/PVPVA, (b) clotrimazole/PVP K29-32 (c) Loratadine/PVPVA, (d) brotrimazole/PVPVA, (e) Me-DIBF/PVPVA.**

4.2 Nuclear Magnetic Resonance Spectroscopy (NMR)

Halogen bonding interactions between components were examined, quantitatively, in solution by NMR spectroscopy by measuring the binding constant between the components. The titration experiments entailed addition of 1-ethyl-2-pyrrolidone (EP), a structural analogue of the repeat unit in the polymers, to a solution of the model compound dissolved in deuterated cyclohexane. Deuterated cyclohexane was chosen as solvent to avoid any potential halogen bonding between π electrons and halogen atoms. For clotrimazole, the ^{1}H NMR spectra showed that the chemical shift of the proton at the para position relative to the chlorine atom changed as a function of EP concentration, as presented in Figure 7S (a). The ^{13}C NMR chemical shift for the carbon atom covalently bonded to the chlorine showed a similar change with addition of EP, as shown in

Figure 7S (b). The change of chemical shift from the ^{1}H and ^{13}C spectra during EP titration is depicted in Figure 4. The binding constant (K_F) values for the halogen bonding interaction between clotrimazole and EP are reported in Table 2 for each nucleus. Similar K_F values were obtained for the halogen bonding interaction from the ^{1}H and ^{13}C NMR titration experiments. Analogous experiments were conducted for brotrimazole and loratadine, and the binding constants are summarized in Table 2. As a negative control, solution ^{1}H NMR of clotrimazole, brotrimazole, and loratadine in the presence of 1-ethylpyrrolidine (no carbonyl group) showed only minor proton shifts (as shown in SI). All the NMR spectra and chemical shift change titration curves are provided in the supporting information. Binding constants were also measured in deuterated toluene (Table S3). It has been reported that π electrons can be halogen bond donors.[53] In toluene, the binding constants were much smaller compared to those in cyclohexane. This is consistent with competition between the toluene π electrons and the carbonyl groups in EP for the halogen atoms. Similar solvent effects have been reported previously.[54] NMR titration experiments were not performed for Me-DIBF due to the complex potential stoichiometry between halogen bond donor and acceptor.

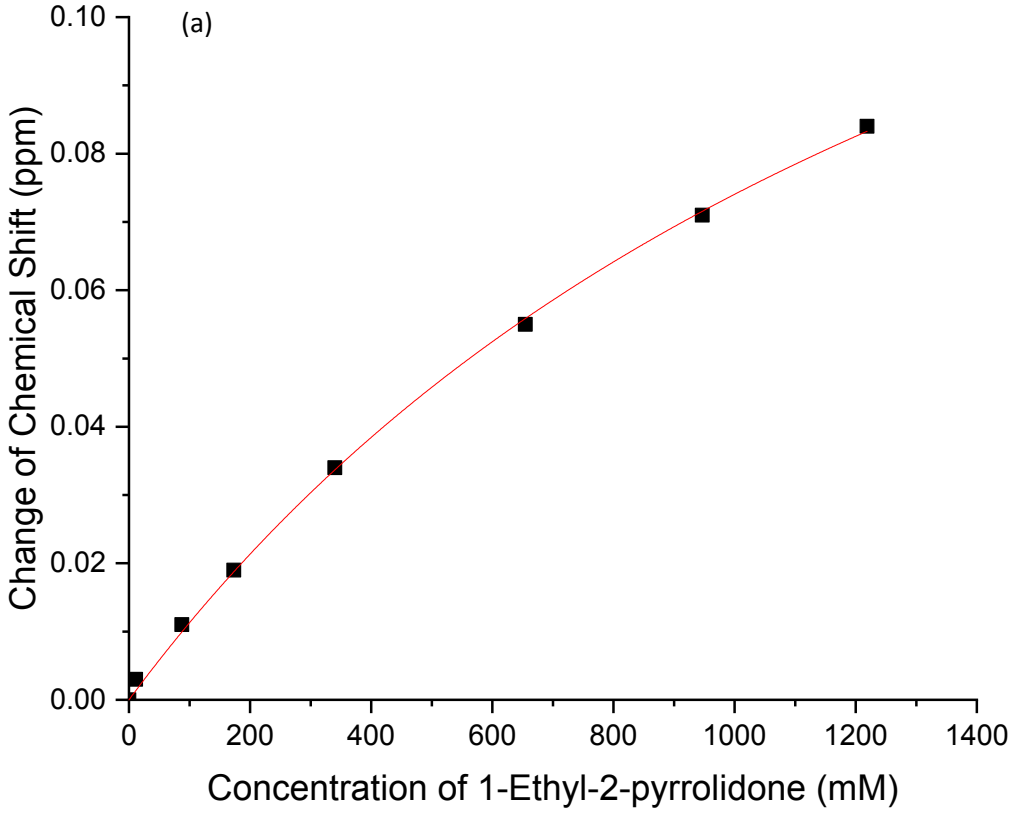
(a)
Change of Chemical Shift (ppm)
0.00
0.02
0.04
0.06
0.08
0.10
0
200
400
600
800
1000
1200
1400
Concentration of 1-Ethyl-2-pyrrolidone (mM)

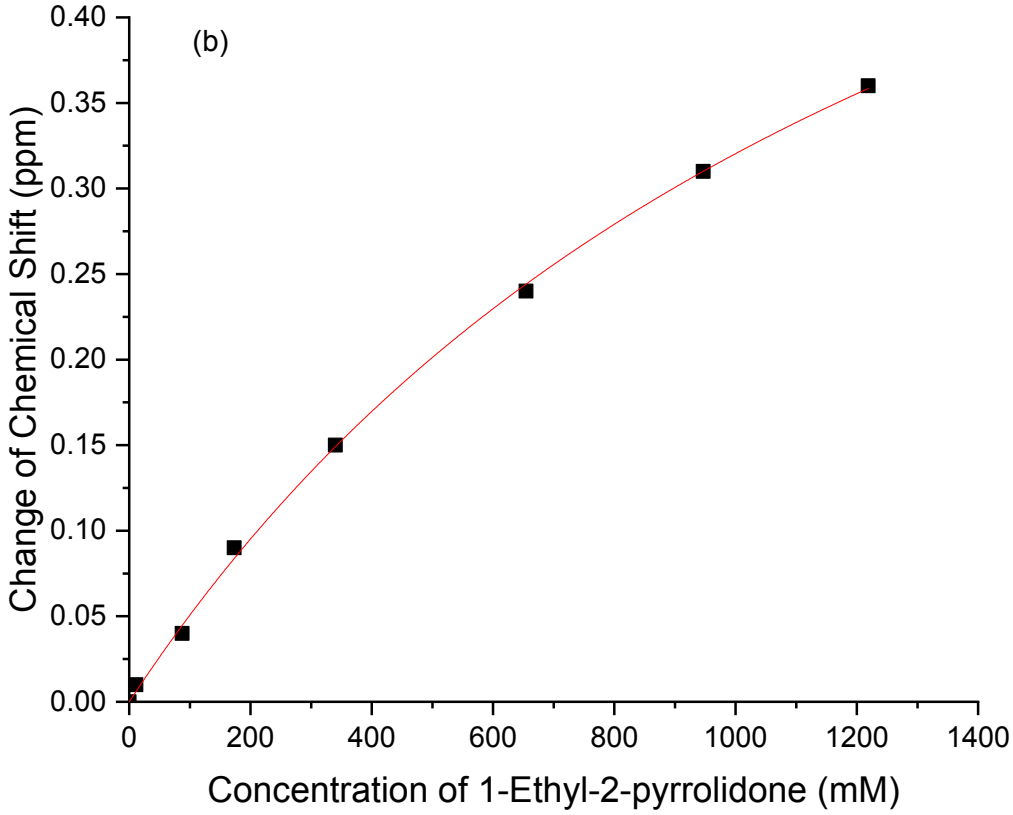

Figure 4. **(a) ^{1}H NMR chemical shift change of clotrimazole as a function of the concentration of 1-ethyl-2-pyrrolidone; (b) ^{13}C NMR chemical shift change of clotrimazole as a function of the concentration of 1-ethyl-2-pyrrolidone.**

Table 2. **K_F values for halogen bonding between model compounds and 1-ethyl-2-pyrrolidone from the ^{1}H and ^{13}C NMR titration experiments at 25 °C in cyclohexane.**

	K_F based on ^{1}H NMR (M^{-1})	K_F based on ^{13}C NMR (M^{-1})
Clotrimazole	0.63 ± 0.05	0.97 ± 0.04
Loratadine	0.65 ± 0.05	1.11 ± 0.07
Brotrimazole	0.56 ± 0.06	0.81 ± 0.04

4.3 Infrared (IR) Spectroscopy of ASDs

IR spectra of PVPVA in the carbonyl region were examined in the absence and presence of molecularly dispersed drug. For pure PVPVA, the peak for the vinylpyrrolidone (VP) carbonyl was around 1684 cm^{-1}, while the position of the vinyl acetate (VA) carbonyl was at 1736 cm^{-1}. The IR spectra for clotrimazole-PVPVA and brotrimazole/PVPVA ASD systems, shown in Figure 5a and 5b respectively, illustrate that the peak maximum corresponding to the carbonyl group in VP shifted slightly to lower wavenumbers, from 1684 cm^{-1} to 1682 cm^{-1}, as the drug loading was increased from 10% to 90%. The spectral shift is well resolved, despite the very small numerical change of only 2 cm^{-1}. The peak position of the carbonyl group in VA did not change. This 2 cm^{-1} shift suggests that the carbonyl group in VP is responsible for the halogen bonding interaction between the model compounds and PVPVA. For Me-DIBF, a similar trend was observed with a larger downshift of 6 cm^{-1}, suggesting stronger halogen bonding interaction in Me-DIBF ASDs.

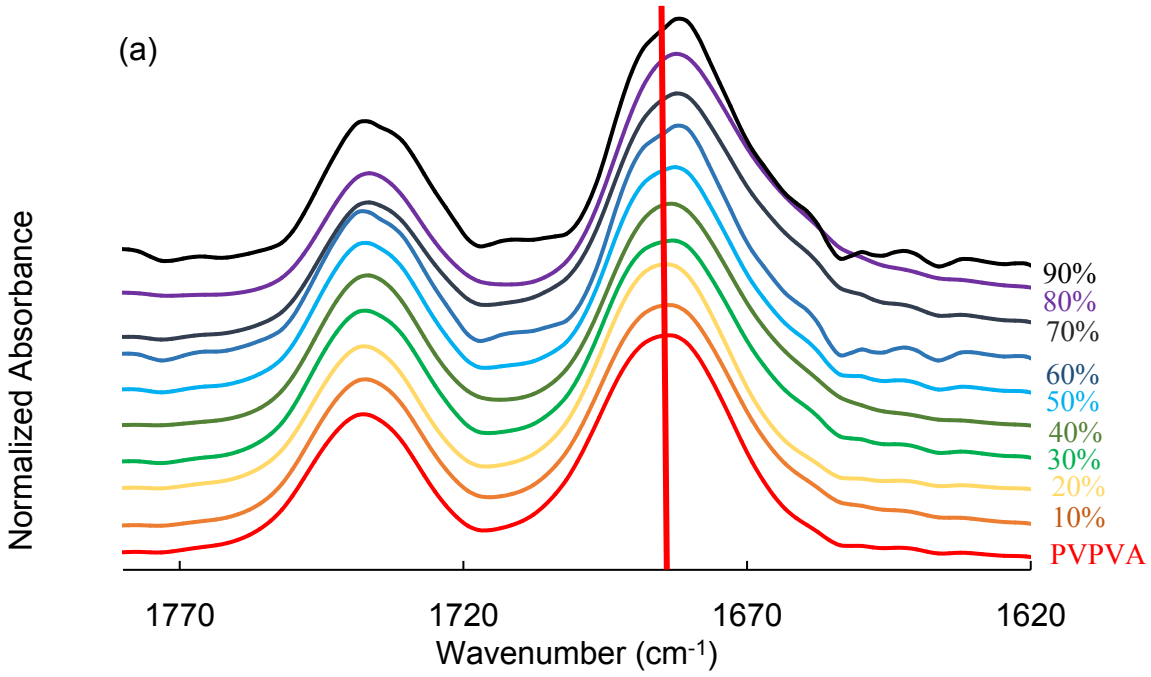

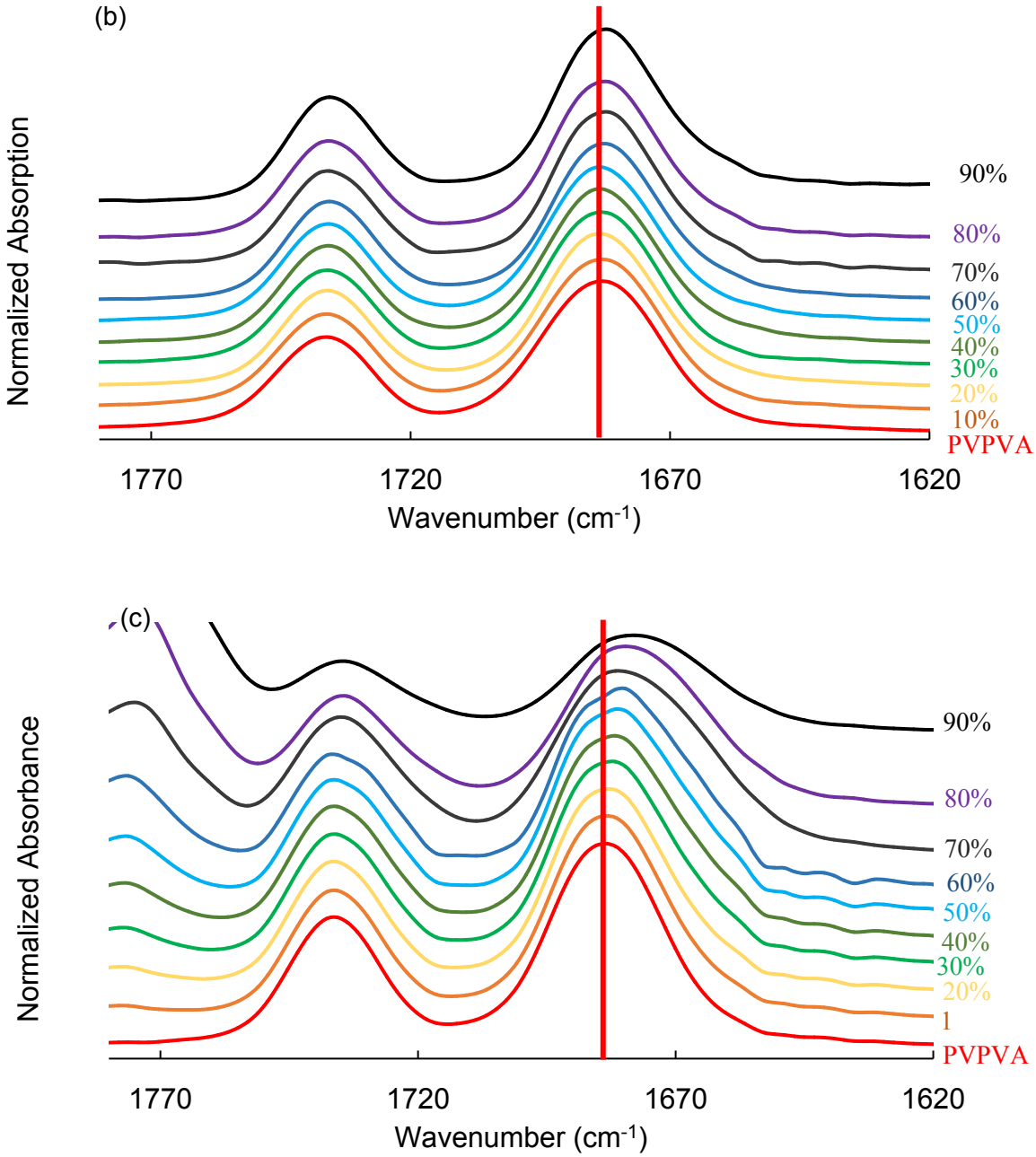

Figure 5. **Infrared spectra of the carbonyl group region of pure PVPVA and (a) clotrimazole-PVPVA ASDs, (b) brotrimazole-PVPVA ASDs, and (c) Me-DIBF-PVPVA ASDs.**

5. Discussion

Halogen bonding (X-bonding) is emerging as an important intermolecular interaction in various areas of science. In the area of drug research, most studies have focused on X-bonding between halogen bearing drugs and proteins, and its role in improving ligand-receptor interactions. As knowledge in this area increases and utilization of halogen groups as a means to enhance drug efficacy becomes more prominent, it becomes increasingly important to understand the relevance of this interaction for other aspects of drug research such as pharmaceutical formulation development. Molecular recognition is of particular importance to the solid state, playing a critical role in both local and long range ordering of materials. In the context of pharmaceutical systems, non-covalent interactions impact properties such as solubility, solid state form landscape, and phase transformations.

Herein, using a variety of orthogonal analytical techniques, we found compelling evidence of X-bonding between drug or drug-like molecules containing Cl, Br, or I but lacking hydrogen bond donors, and polymers, such as PVPVA and PVP. XPS appears to be of particular utility for studying changes in the halogen environment, being one of the few techniques that allow a direct probe of the halogen moiety. Further, photoelectron spectra are sensitive to intermolecular interactions. For example, ionic and hydrogen bond interactions are well known to lead to binding energy shifts in the photoelectron spectra.[55, 56] Thus, we note that the binding energies of Cl 2p, Br 3d, and I 3d peaks decreased when the model compounds were molecularly dispersed in PVPVA. The lowering of the binding energy indicates that these halogen atoms gain electron density when the polymer is present. This trend is consistent with halogen bonding, where the σ-hole on the halogen atom is known to attract electrons. Moreover, the 2-4 eV binding energy shift observed is significant and comparable to the binding energy shift produced by hydrogen

bonding.[56] This lends support that the shift is due to a specific intermolecular interaction. Shifts to a lower binding energy, albeit to a lesser extent, have been reported for systems containing halogen bonds between iodine atoms and nitrogen,[57, 58] providing further support to our interpretation. Oxygen in carbonyl is known to be one of the most common halogen bond acceptors, in particular for protein-ligand interactions.[14] Further, it is well-known that the amide carbonyl group of the vinyl pyrrolidone group in PVP and PVPVA is a good hydrogen bond acceptor.[41] Therefore, it is not surprising that this group acts as the halogen bond acceptor. Results from IR spectroscopy confirm that the vinyl pyrrolidone group is preferred relative to the vinyl acetate group (Figure 5). Further support for the supposition that this oxygen group donates electrons to the halogen atom is provided by examination of the O1s peak of PVP in the presence and absence of clotrimazole. For all other systems, XPS spectra contain signal from multiple oxygen atoms, however, for the PVP-clotrimazole system the O1s peak arises solely from the vinylpyrrolidone carbonyl. In the dispersion, the O1s binding energy shifts to a higher value by 0.2 eV relative to neat PVP (Figure 6S), suggesting a reduction in electron density consistent with the formation of a halogen bond. The minimal change in the ^{1}H NMR spectrum of clotrimazole, brotrimazole and loratadine in the presence of 1-ethylpyrrolidine (which lacks a carbonyl group) relative to the large shifts seen in the presence of the carbonyl containing analogue 1-ethyl-2-pyrrolidone, further supports the role of the VP oxygen as the halogen bond acceptor. Halogen bonding with a carbonyl group has also been seen not only in protein-ligand binding,[59, 60] but also between two small molecules.[23, 24] In summary, based on the evidence presented herein, we propose that halogen bonding exists between the amide carbonyl , on the polymer, and halogen atoms, Cl, Br, or I, in ASDs. In addition, the interaction occurs to a greater extent when the drug loading is low and drug-drug intermolecular interactions are less probable.

Halogen bonds share many similar characteristics with the more commonly encountered hydrogen bonds. They are both directional interactions between an electron-deficient moiety and a high electron density region. They are similar in the strength of interaction. The binding energy for hydrogen bonding is 0.2 to 40 kcal/mol, while for halogen bonding it is 1.2 to 43 kcal/mol.[61, 62] Therefore, the interaction strengths of halogen and hydrogen bonds can be comparable. Specifically for the systems we have studied here, the halogen bond strength between the compounds and PVPVA appears to be similar to weak hydrogen bonding interactions. The binding constants, which reflects the strength of interaction, between clotrimazole, brotrimazole, and loratadine with EP (Table 2) are between 0.6-1.1 M^{-1}. They are of similar magnitude as the 0.7 M^{-1} binding constant corresponding to weak hydrogen bonds, where fluorine is the hydrogen bond acceptor.[51] The IR carbonyl absorption peak only shifted 2-6 cm^{-1} when halogen bonded to the model compounds in the ASDs. In contrast, red shifts as large as 20-30 cm^{-1} have been observed when PVP forms hydrogen bonds with drugs in ASDs.[9, 63, 64] In general, the strength of halogen bonds correlate with the polarizability of the halogen atoms, following the trend I > Br > Cl. In our study, however, we have observed similar interaction strength between of -Cl and -Br analogues, based on the binding constant measured from the NMR titration and the wavenumber shift in the IR absorption of the carbonyl group. This observation can perhaps be rationalized based on analysis of cohesive interactions in the crystal. In brotrimazole, there is intermolecular interaction between Br and either the phenyl group or imidazole, however, this interaction was not observed in the clotrimazole crystal. Thus, the tendency for brotrimazole to self-interact may be greater compared to clotrimazole, and this interaction can compete with the brotrimazole-PVPVA intermolecular interaction. The formation of halogen bonds with phenyl groups is further suggested by the smaller binding constants between model compounds and EP in toluene

(Tablet S3), where the π electrons of the solvent molecules can compete with carbonyl groups of EP as halogen bond donors. For Me-DIBF/PVPVA ASDs, the carbonyl moiety showed larger IR shift, suggesting stronger halogen bonding.

A comparison of the extent of interaction between the various compounds and the polymer carbonyl is shown in Figure 6. Here, the ratio of free-to-halogen bonded VP carbonyls is compared as a function of the amount of compound added. At lower drug loading, there is an excess of carbonyl groups available for halogen bonding and the drug-polymer interaction is undersaturated. As the drug load increases, a maximum of about 1 halogen bonded carbonyl per 8 free carbonyls is observed, with no further decreases when additional amounts of drug are present. This saturation may be due, at least in part, to steric constraints. Interestingly, the drug-polymer interaction saturates at approximately the same ratio of free carbonyls to halogen bonded carbonyls (y axis in Figure 6) for all systems with increases in drug load, which further suggests possible steric constraints. Halogen bonding extent did not increase when Cl was replaced with Br, as corroborated by NMR titration results (Table 2). The iodine-containing compound, Me-DIBF, contains four iodine groups per molecule, and multiple halogen bonds can be formed for each molecule, likely leading to the observed rapid saturation.

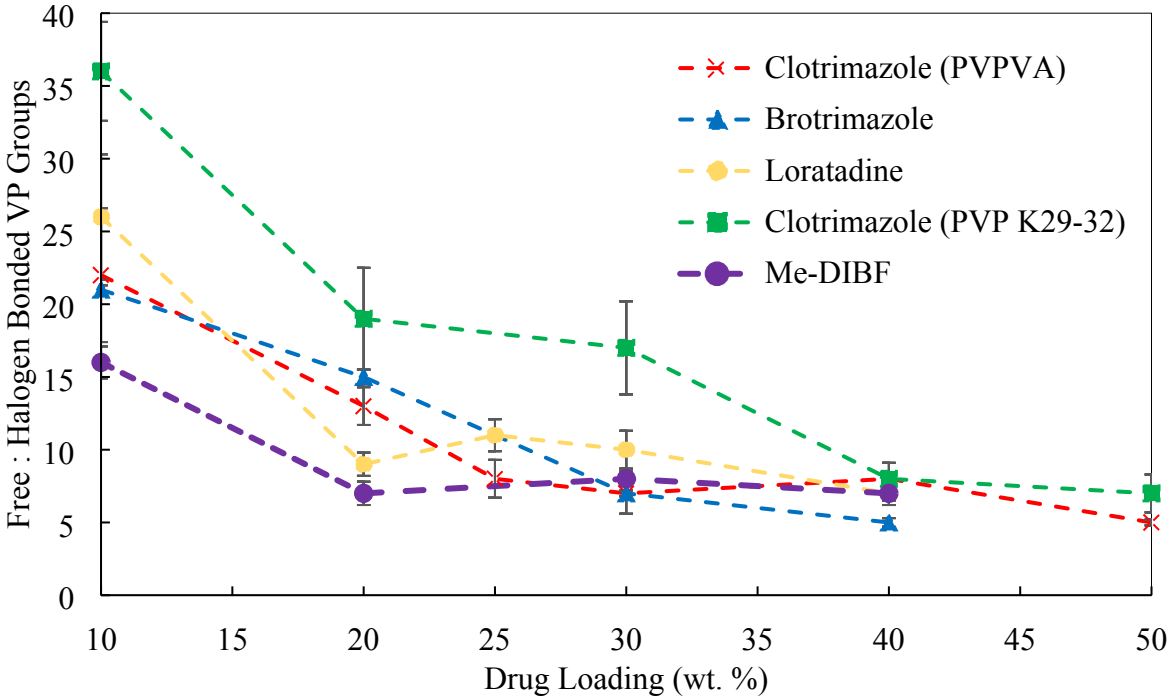

Figure 6. **Molar ratio of free:halogen bonded vinyl-2-pyrrolidinone moieties as a function of drug loading. The dotted line is shown as a visual guide. The number of VP carbonyl groups acting as halogen bond acceptors is considered equal to the number of halogen atoms participating in halogen bonding (Fig. 3).**

6. Conclusions

The halogen-containing molecules studied, namely clotrimazole, loratadine, brotrimazole, and Me-DIBF, were found to form halogen bonds with the amide carbonyl of the vinylpyrrolidone moiety in copovidone-based amorphous dispersions. This is the first time that the presence of halogen bonding has been reported in drug-polymer blends. Orthogonal spectroscopic techniques, specifically IR, NMR and XPS spectroscopy, showed peak shifts consistent with the transfer of electrons from the oxygen atom on the polymer to the halogen atoms on drugs. Based on IR spectroscopic data, iodine appeared to form a stronger interaction than either Cl or Br, which appeared similar in strength. The results from this study serve to highlight the occurrence of this common, but long-neglected intermolecular interaction in drug-polymer formulations.

With the increasing utilization of halogen atoms in drug design to enhance pharmacological performance, the potential impact of halogen bonding on formulation performance warrants further investigation and exploration.

Disclosure

Purdue University and AbbVie jointly participated in study design, research, data collection, analysis and interpretation of data, writing, reviewing, and approving the publication. Chailu Que and Alexandru Deac are graduate students at Purdue University. Qingqing Qi is a postdoctoral associate at Purdue University. Lynne S. Taylor is a professor at Purdue University. Huaping Mo and Dmitry Zemlyanov and Matthias Zeller are research scientists at Purdue University. They all have no additional conflicts of interest to report. Anura S. Indulkar, Yi Gao, and Geoff G. Z. Zhang are employees of AbbVie and may own AbbVie stock.

Supporting Information

^{1}H and ^{13}C NMR spectra of brotrimazole, ^{1}H and ^{13}C NMR spectra of Me-DIBF, X-ray crystallography of brotrimazole, X-ray photoelectron spectroscopy of ASDs, Nuclear Magnetic Resonance Spectroscopy titration data for clotrimazole, brotrimazole and loratadine, binding constants in toluene. This material is available free of charge via the internet at http://pubs.acs.org.

Acknowledgement

We would like to acknowledge AbbVie Inc. for providing research funding for this project. The single crystal X-ray diffractometer is supported by the National Science Foundation through the Major Research Instrumentation Program under Grant No. CHE 1625543.

References

(1) Gardner, C. R.; Walsh, C. T.; Almarsson, Ö. Drugs as Materials: Valuing Physical Form in Drug Discovery. *Nat. Rev. Drug Discov.* **2004,** *3*, 926.
(2) Lipinski, C. A. Drug-like Properties and the Causes of Poor Solubility and Poor Permeability. *J. Pharmacol. Toxicol. Methods* **2000,** *44*, 235-249.
(3) Law, D.; Schmitt, E. A.; Marsh, K. C.; Everitt, E. A.; Wang, W.; Fort, J. J.; Krill, S. L.; Qiu, Y. Ritonavir–PEG 8000 Amorphous Solid Dispersions: In vitro and In vivo Evaluations. *J. Pharm. Sci.* **2004,** *93*, 563-570.
(4) Wilson, V.; Lou, X.; Osterling, D. J.; Stolarik, D. F.; Jenkins, G.; Gao, W.; Zhang, G. G. Z.; Taylor, L. S. Relationship between Amorphous Solid Dispersion in vivo Absorption and in vitro Dissolution: Phase Behavior during Dissolution, Speciation, and Membrane Mass Transport. *J. Control. Release* **2018,** *292*, 172-182.
(5) Chan, S. Y.; Qi, S.; Craig, D. Q. An Investigation into the Influence of Drug-polymer Interactions on the Miscibility, Processability and Structure of Polyvinylpyrrolidone-based Hot Melt Extrusion Formulations. *Int. J. Pharm.* **2015,** *496*, 95-106.
(6) Chen, Y.; Chen, H.; Wang, S.; Liu, C.; Qian, F. A Single Hydrogen to Fluorine Substitution Reverses the Trend of Surface Composition Enrichment of Sorafenib Amorphous Solid Dispersion upon Moisture Exposure. *Pharm. Res.* **2019,** *36*, 105.
(7) Frank, D. S.; Matzger, A. J. Probing the Interplay between Amorphous Solid Dispersion Stability and Polymer Functionality. *Mol. Pharm.* **2018,** *15*, 2714-2720.
(8) Huang, J.; Wigent, R. J.; Schwartz, J. B. Drug-polymer Interaction and Its Significance on the Physical Stability of Nifedipine Amorphous Dispersion in Microparticles of an Ammonio Methacrylate Copolymer and Ethylcellulose Binary Blend. *J. Pharm. Sci.* **2008,** *97*, 251-262.
(9) Rumondor, A. C. F.; Marsac, P. J.; Stanford, L. A.; Taylor, L. S. Phase Behavior of Poly(vinylpyrrolidone) Containing Amorphous Solid Dispersions in the Presence of Moisture. *Mol. Pharm.* **2009,** *6*, 1492-1505.
(10) Taylor, L. S.; Zografi, G. Spectroscopic characterization of interactions between PVP and indomethacin in amorphous molecular dispersions. *Pharm. Res.* **1997,** *14*, 1691-1698.
(11) Miyazaki, T.; Yoshioka, S.; Aso, Y.; Kojima, S. Ability of polyvinylpyrrolidone and polyacrylic acid to inhibit the crystallization of amorphous acetaminophen. *J. Pharm. Sci.* **2004,** *93*, 2710-2717.
(12) Yokoi, Y.; Yonemochi, E.; Terada, K. Effects of sugar ester and hydroxypropyl methylcellulose on the physicochemical stability of amorphous cefditoren pivoxil in aqueous suspension. *Int. J. Pharm.* **2005,** *290*, 91-99.
(13) Cavallo, G.; Metrangolo, P.; Milani, R.; Pilati, T.; Priimagi, A.; Resnati, G.; Terraneo, G. The Halogen Bond. *Chem. Rev* **2016,** *116*, 2478-2601.
(14) Xu, Z.; Yang, Z.; Liu, Y.; Lu, Y.; Chen, K.; Zhu, W. Halogen bond: its role beyond drug-target binding affinity for drug discovery and development. *J. Chem. Inf. Model.* **2014,** *54*, 69-78.
(15) Shinada, N. K.; de Brevern, A. G.; Schmidtke, P. Halogens in Protein-Ligand Binding Mechanism: A Structural Perspective. *J. Med. Chem.* **2019,** *62*, 9341-9356.
(16) Hassel, O. Structural Aspects of Interatomic Charge-Transfer Bonding. *Science* **1970,** *170* (3957), 497-502.
(17) Zordan, F.; Brammer, L.; Sherwood, P. Supramolecular Chemistry of Halogens: Complementary Features of Inorganic (M−X) and Organic (C−X') Halogens Applied to M−X···X'−C Halogen Bond Formation. *J. Am. Chem. Soc.* **2005,** *127*, 5979-5989.
(18) Aakeroy, C. B.; Spartz, C. L.; Dembowski, S.; Dwyre, S.; Desper, J. A Systematic Structural Study of Halogen Bonding versus Hydrogen Bonding within Competitive Supramolecular Systems. *IUCrJ* **2015,** *2*, 498-510.
(19) Gilles Berger; Jalal Soubhyea; Meyer, F. Halogen Bonding in Polymer Science: From Crystal Engineering to Functional Supramolecular Polymers and Materials. *Polym. Chem* **2015,** *6*, 3559-3580.

(20) Hardegger, L. A.; Kuhn, B.; Spinnler, B.; Anselm, L.; Ecabert, R.; Stihle, M.; Gsell, B.; Thoma, R.; Diez, J.; Benz, J.; Plancher, J. M.; Hartmann, G.; Banner, D. W.; Haap, W.; Diederich, F. Systematic investigation of halogen bonding in protein-ligand interactions. *Angew. Chem. Int. Ed.* **2011,** *50*, 314-318.
(21) Sirimulla, S.; Bailey, J. B.; Vegesna, R.; Narayan, M. Halogen Interactions in Protein–Ligand Complexes: Implications of Halogen Bonding for Rational Drug Design. *J. Chem. Inf. Model.* **2013,** *53*, 2781-2791.
(22) Meazza, L.; Foster, J. A.; Fucke, K.; Metrangolo, P.; Resnati, G.; Steed, J. W. Halogen-bonding-triggered Supramolecular Gel Formation. *Nat. Chem.* **2013,** *5*, 42.
(23) Gliese, J. P.; Jungbauer, S. H.; Huber, S. M. A halogen-bonding-catalyzed Michael addition reaction. *ChemComm* **2017,** *53*, 12052-12055.
(24) Jungbauer, S. H.; Walter, S. M.; Schindler, S.; Rout, L.; Kniep, F.; Huber, S. M. Activation of a carbonyl compound by halogen bonding. *ChemComm* **2014,** *50*, 6281-6284.
(25) Lahtinen, M.; Kolehmainen, E.; Haarala, J.; Shevchenko, A. Evidence of weak halogen bonding: New insights on itraconazole and its succinic acid cocrystal. *Cryst. Growth Des.* **2013,** *13*, 346-351.
(26) Choquesillo-Lazarte, D.; Nemec, V.; Cinčić, D. Halogen bonded cocrystals of active pharmaceutical ingredients: pyrazinamide, lidocaine and pentoxifylline in combination with haloperfluorinated compounds. *CrystEngComm* **2017,** *19*, 5293-5299.
(27) Baldrighi, M.; Cavallo, G.; Chierotti, M. R.; Gobetto, R.; Metrangolo, P.; Pilati, T.; Resnati, G.; Terraneo, G. Halogen bonding and pharmaceutical cocrystals: the case of a widely used preservative. *Mol. Pharm.* **2013,** *10*, 1760-1772.
(28) Metrangolo, P.; Murray, J. S.; Pilati, T.; Politzer, P.; Resnati, G.; Terraneo, G. Fluorine-Centered Halogen Bonding: A Factor in Recognition Phenomena and Reactivity. *Cryst. Growth Des.* **2011,** *11*, 4238-4246.
(29) Wilcken, R.; Zimmermann, M. O.; Lange, A.; Joerger, A. C.; Boeckler, F. M. Principles and applications of halogen bonding in medicinal chemistry and chemical biology. *J. Med. Chem.* **2013,** *56*, 1363-1388.
(30) Riley, K. E.; Hobza, P. Strength and Character of Halogen Bonds in Protein–Ligand Complexes. *Cryst. Growth Des.* **2011,** *11*, 4272-4278.
(31) Lommerse, J. P.; Price, S. L.; Taylor, R. Hydrogen bonding of carbonyl, ether, and ester oxygen atoms with alkanol hydroxyl groups. *J. Comput. Chem.* **1997,** *18*, 757-774.
(32) Christer B. Aakeröy; Meg Fasulo; Nate Schultheiss; John Desper; Moore, C. Structural Competition between Hydrogen Bonds and Halogen Bonds. *J. Am. Chem. Soc.* **2007,** *129*, 13772-13773.
(33) Robertson, C. C.; Wright, J. S.; Carrington, E. J.; Perutz, R. N.; Hunter, C. A.; Brammer, L. Hydrogen bonding vs. halogen bonding: the solvent decides. *Chem. Sci.* **2017,** *8* (8), 5392-5398.
(34) Nemec, V.; Fotović, L.; Friščić, T.; Cinčić, D. A Large Family of Halogen-Bonded Cocrystals Involving Metal–Organic Building Blocks with Open Coordination Sites. *Cryst. Growth Des.* **2017,** *17*, 6169-6173.
(35) Xu, Y.; Viger-Gravel, J.; Korobkov, I.; Bryce, D. L. Mechanochemical Production of Halogen-Bonded Solids Featuring P═O • • • I ⁻ C Motifs and Characterization via X-ray Diffraction, Solid-State Multinuclear Magnetic Resonance, and Density Functional Theory. *J. Phys. Chem. C* **2015,** *119*, 27104-27117.
(36) Laurence, C.; Queignec-Cabanetos, M.; Dziembowska, T.; Queignec, R.; Wojtkowiak, B. 1-Iodoacetylenes. 1. Spectroscopic evidence of their complexes with Lewis bases. A spectroscopic scale of soft basicity. *J. Am. Chem. Soc.* **1981,** *103*, 2567-2573.
(37) M.T. Messina; P. Metrangolo; W. Navarrini; S. Radice; G. Resnati; Zerbi, G. Infrared and Raman Analyses of the Halogen-bonded Non-covalent Adducts Formed by a,v-diiodoperfluoroalkanes with DABCO and Other Electron Donors. *J. Mol. Struct.* **2000,** *524,* 87-94.

(38) Poleshchuk, O. K.; Branchadell, V.; Brycki, B.; Fateev, A. V.; Legon, A. C. HFI and DFT Study of the Bonding in Complexes of Halogen and Interhalogen Diatomics with Lewis Base. *Comput. Theor. Chem.* **2006,** *760*, 175-182.
(39) Liao, J. J.-L. Molecular recognition of protein kinase binding pockets for design of potent and selective kinase inhibitors. *J. Med. Chem.* **2007,** *50*, 409-424.
(40) Rumondor, A. C. F.; Dhareshwar, S. S.; Kesisoglou, F. Amorphous Solid Dispersions or Prodrugs: Complementary Strategies to Increase Drug Absorption. *J. Pharm. Sci.* **2016,** *105*, 2498-2508.
(41) Yuan, X.; Xiang, T. X.; Anderson, B. D.; Munson, E. J. Hydrogen Bonding Interactions in Amorphous Indomethacin and Its Amorphous Solid Dispersions with Poly(vinylpyrrolidone) and Poly(vinylpyrrolidone-co-vinyl acetate) Studied Using (13)C Solid-State NMR. *Mol. Pharm.* **2015,** *12*, 4518-4528.
(42) Mistry, P.; Mohapatra, S.; Gopinath, T.; Vogt, F. G.; Suryanarayanan, R. Role of the strength of drug–polymer interactions on the molecular mobility and crystallization inhibition in ketoconazole solid dispersions. *Mol. Pharm.* **2015,** *12*, 3339-3350.
(43) Lu, X.; Huang, C.; Lowinger, M. B.; Yang, F.; Xu, W.; Brown, C. D.; Hesk, D.; Koynov, A.; Schenck, L.; Su, Y. Molecular Interactions in Posaconazole Amorphous Solid Dispersions from Two-Dimensional Solid-State NMR Spectroscopy. *Mol. Pharm.* **2019,** *16*, 2579-2589.
(44) Shoichet, B. K.; Stroud, R. M.; Santi, D. V.; Kuntz, I. D.; Perry, K. M. Structure-based discovery of inhibitors of thymidylate synthase. *Science* **1993,** *259*, 1445-1450.
(45) Cai, F.; Pu, X.; Qi, X.; Lynch, V.; Radha, A.; Ready, J. M. Chiral Allene-Containing Phosphines in Asymmetric Catalysis. *J. Am. Chem. Soc.* **2011,** *133*, 18066-18069.
(46) *SHELXTL suite of programs, Version 6.14, 2000-2003, Bruker Advanced X-ray Solutions, Bruker AXS Inc., Madison, Wisconsin: USA*
(47) Sheldrick, G. M. A short history of SHELX. *Acta Crystallographica Section A: Foundations of Crystallography* **2008,** *64*, 112-122.
(48) Sheldrick, G. M. University of Göttingen, 2018.
(49) Sheldrick, G. M. Crystal structure refinement with SHELXL. *Acta Crystallographica Section C: Structural Chemistry* **2015,** *71*, 3-8.
(50) Gurka, D.; Taft, R. W. Studies of Hygeon-Bonded Complex Formation with p-Fluorophenol. IV. The Fluorine Nuclear Magnetic Resonance Method. *J. Am. Chem. Soc.* **1969,** *91*, 4794-4801.
(51) Dalvit, C.; Vulpetti, A. Weak Intermolecular Hydrogen Bonds with Fluorine: Detection and Implications for Enzymatic/Chemical Reactions, Chemical Properties, and Ligand/Protein Fluorine NMR Screening. *Chem.: Eur. J.* **2016,** *22*, 7592-7601.
(52) Thordarson, P. Determining Association Constants from Titration Experiments in Supramolecular Chemistry. *Chem. Soc. Rev.* **2011,** *40*, 1305-1323.
(53) Politzer, P.; Murray, J. S.; Clark, T. Halogen bonding: an electrostatically-driven highly directional noncovalent interaction. *Phys. Chem. Chem. Phys.* **2010,** *12*, 7748-7757.
(54) Ma, N.; Zhang, Y.; Ji, B.; Tian, A.; Wang, W. Structural Competition between Halogen Bonds and Lone‐Pair⋯π Interactions in Solution. *ChemPhysChem* **2012,** *13*, 1411-1414.
(55) Zhou, X.; Goh, S. H.; Lee, S. Y.; Tan, K. L. X-ray Photoelectron Spectroscopic Studies of Interactions between Poly(p-vinylphenol) and Poly(vinylpyridine)s. *Appl. Surf. Sci.* **1997,** *119*, 60-66.
(56) Cecchet, F.; Rudolf, P.; Rapino, S.; Margotti, M.; Paolucci, F.; Baggerman, J.; Brouwer, A. M.; Kay, E. R.; Wong, J. K. Y.; Leigh, D. A. Structural, Electrochemical, and Photophysical Properties of a Molecular Shuttle Attached to an Acid-Terminated Self-Assembled Monolayer. *J. Phys. Chem. B* **2004,** *108*, 15192-15199.
(57) Wang, F.; Ma, N.; Chen, Q.; Wang, W.; Wang, L. Halogen bonding as a new driving force for layer-by-layer assembly. *Langmuir* **2007,** *23*, 9540-9542.

(58) Xu, J.; Liu, X.; Ng, J. K.-P.; Lin, T.; He, C. Trimeric supramolecular liquid crystals induced by halogen bonds. *J. Mater. Chem.* **2006,** *16,* 3540-3545.
(59) Himmel, D. M.; Das, K.; Clark, A. D.; Hughes, S. H.; Benjahad, A.; Oumouch, S.; Guillemont, J.; Coupa, S.; Poncelet, A.; Csoka, I. Crystal structures for HIV-1 Reverse Transcriptase in Complexes with Three Pyridinone Derivatives: a New Class of Non-nucleoside Inhibitors Effective Against a Broad Range of Drug-resistant Strains. *J. Med. Chem.* **2005,** *48*, 7582-7591.
(60) Riley, K. E.; Murray, J. S.; Politzer, P.; Concha, M. C.; Hobza, P. Br...O Complexes as Probes of Factors Affecting Halogen Bonding: Interactions of Bromobenzenes and Bromopyrimidines with Acetone. *J. Chem. Theory Comput.* **2009,** *5*, 155-163.
(61) Steiner, T. The Hydrogen Bond in the Solid State. *Angew. Chem. Int. Ed.* **2002,** *41*, 48-76.
(62) Metrangolo, P.; Neukirch, H.; Pilati, T.; Resnati, G. Halogen Bonding based Recognition Processes: a World Parallel to Hydrogen Bonding. *Acc. Chem. Res.* **2005,** *38*, 386-395.
(63) Wegiel, L. A.; Mauer, L. J.; Edgar, K. J.; Taylor, L. S. Mid-infrared spectroscopy as a polymer selection tool for formulating amorphous solid dispersions. *J. Pharm. Pharmacol.* **2014,** *66*, 244-255.
(64) Kestur, U. S.; Van Eerdenbrugh, B.; Taylor, L. S. Influence of polymer chemistry on crystal growth inhibition of two chemically diverse organic molecules. *CrystEngComm* **2011,** *13*, 6712-6718.

For Table of Contents Use Only

Evidence for Halogen Bonding in Amorphous Solid Dispersions

Chailu Que, Qingqing Qi, Dmitry Y. Zemlyanov, Huaping Mo, Alexandru Deac, Matthias Zeller, Anura S. Indulkar, Yi Gao, Geoff G. Z. Zhang, and Lynne S. Taylor

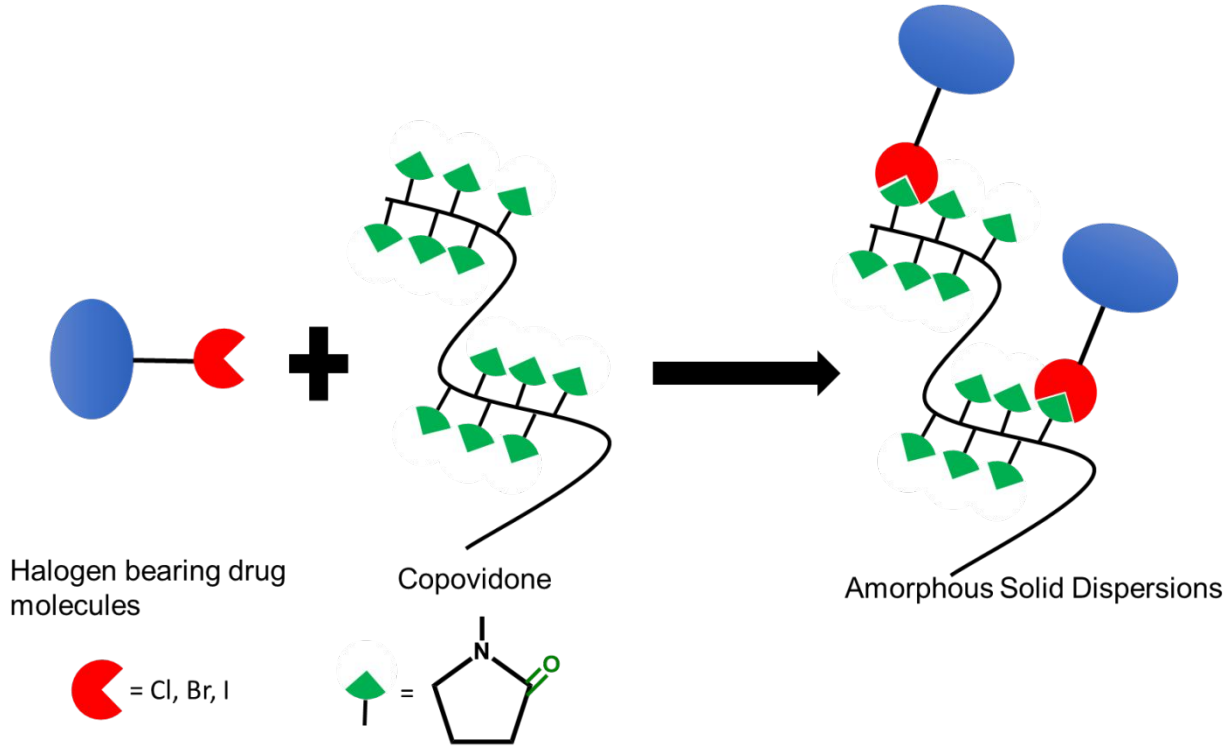

Halogen bonds were found to occur between drug molecules containing Cl, Br or I and the carbonyl group of copovidone, in amorphous drug-polymer blends.